A Lipidated Peptide with Mitochondrial Membrane Localization in Human A549 Lung Cells: From Enhanced Cell-Penetrating Properties to Biological Activity Mechanism

Xinlei Zhang, Angelina Angelova, Wanfeng Sun, Fan Zhang, Na Li, Aihua Zou

A Lipidated Peptide with Mitochondrial Membrane Localization in Human A549 Lung Cells: From Enhanced Cell-Penetrating Properties to Biological Activity Mechanism

Xinlei Zhang[a], Angelina Angelova[c], Fan Zhang[a],

Na Li[d*], and Aihua Zou[a,b*]

[a]Shanghai Key Laboratory of Functional Materials Chemistry, State Key Laboratory of Bioreactor Engineering and Institute of Applied Chemistry, School of Chemistry and Molecular Engineering, East China University of Science and Technology, Shanghai 200237, P.R. China

[b]College of Chemistry and Materials Science, Shanghai Normal University, Shanghai 200234, P. R. China

[c]Université Paris-Saclay, CNRS, Institut Galien Paris-Saclay UMR8612, F-92296 Châtenay-Malabry, France

[d]National Facility for Protein Science in Shanghai Zhangjiang Laboratory, Shanghai Advanced Research Institute, CAS, No.333, Haike Road, Shanghai 20124, P.R. China

***Corresponding author**
Email: aihuazou@shnu.edu.cn (Aihua Zou);

nli@sibcb.ac.cn (Na Li)

ABSTRACT: Here a lipidated peptide Pal-pHK-pKV with self-assembly properties and ability to provoke the disruption of the mitochondrial voltage-dependent anion channel-1 protein (VDAC1)-Hexokinase-II (HK-II) complex is reported. The effects of the peptide pHK (N-terminal 15-amino acid fragment of HK-II that specifically binds VDAC1) are compared with those of a designed biomimetic amphiphilic pHK-pKV conjugate (pHK coupled with a new cell penetrating peptide pKV) and Pal-pHK-pKV (a lipidated conjugate modified with a hydrophobic palmitic (Pal) alkyl chain). The Pal-pHK-pKV exhibits stronger interaction with the membrane as compared to pHK-pKV, which is demonstrated by Langmuir-Blodgett technique and two-photon excitation microscopy. The amphiphilic peptide derivatives are cytotoxic to the A549 cells, but Pal-pHK-pKV is more cytotoxic. The inhibitory effects of the pHK derivatives on the A549 cells growth are investigated through induced apoptosis pathway, depolarized mitochondrial membrane potential, and activated caspase. The results of the immunofluorescence evidence the specific mitochondrial targeting by those derivatives.

Keywords: lipidated mitochondria-targeting peptide; vibration-induced emission; cell penetrating peptide; mitochondrial membrane potential; A549 cells

1. Introduction

Lung cancer is a severe malignancy for the respiratory system, for which non-small cell lung cancer (NSCLC) is the leading cause of death.[1-3] The growth and division of the malignant cells of squamous cell carcinoma, adenocarcinoma and large-cell carcinoma type occur at relatively late stages of metastasis in NSCLC.[4] Diverse treatments of NSCLC include lesion resection[5], radiotherapy[6], chemotherapy[7] and targeted therapies[8-10], which are

least invasive. Small molecular drugs, such as gefitinib[11], erlotinib[12], doxorubicin[13], paclitaxel[14], and cisplatin[15], have been largely tested against NSCLC. However, they have found limited application in clinics owing to drug resistance, side effects, and high price.

In recent years, mitochondria-mediated apoptosis receives considerable attention in the development of targeted and combination therapies against cancer.[16-25] Sorafenib, 4-Methylsulfinyl-3-butenyl isothiocyanate, and calpeptin are selected examples of therapeutic agents, which act on protein targets located in the outer or the inner mitochondrial membranes. These small molecule drugs directly acting on the mitochondria-mediated apoptosis, or drugs which can be used in combination therapies based on complimentary biological mechanisms aiming at cancer inhibition.

Protein mimetic peptide amphiphiles and hybrid lipidated peptide conjugates, obtained by anchoring of hydrophobic moieties and cell-penetrating amino-acid sequences to anticancer peptides, represent a promising emergent strategy for cancer inhibition.[16-22, 25] Peptides may exert excellent anti-tumor activity and appropriate physico-chemical properties, which ensure their potential as anticancer drug candidates. At variance to traditional low molecular weight compounds, peptide drugs exhibit good biocompatibility, specificity in tumor targeting, and high drug efficacy.[26, 27] Moreover, peptides with cell-penetrating properties (CPP) can be used as nanocarriers for delivery of proteins, vaccines, antibodies, and small molecular drugs causing cancer cell apoptosis. Thus, they have strong effects on tumor cell proliferation.[28, 29]

Peptide drugs may cause cancer cell apoptosis *via* at least two ways (i) endogenous mitochondrial pathway, and (ii) exogenous death receptor pathway.[30] The Bcl-2 protein

family controls the endogenous mitochondrial pathway,[31] which plays a key role in the cell apoptosis process. The protein Bax binds to the voltage-dependent anion channel-1 protein (VDAC1), leading to high conductivity channels formation in the cell membrane, which results in cytochrome c (Cyt-c) release. However, the binding between Bax and VDAC1 can be blocked in the presence of Hexokinase II (HK-II),[32, 33] which favours the growth of tumor cells. HK-II, which is normally expressed in the mitochondrion of healthy cells, is overexpressed in the mitochondrion of tumor cells.[34] In aggressive tumors with high glycolytic action, the activity of mitochondrial HK-II increases synergistically, which has been defined as Warburg effect.[35] The over-expressed HK-II enzyme converts glucose into glucose-6-phosphate.

The VDAC1, located on the outer mitochondrial membrane, can interact with more than 100 proteins in the cells, participate in cell metabolism and apoptosis, and has become the target of many pathological treatments including cancer.[36] Among them, the N-terminal 15 amino acid fragment (pHK) of the HK-II (MIASHLLAYFFTELN) binds VDAC1 at the outer mitochondrial membrane forming a complex VDAC1-HK-II. This prevents the release of Cyt-c from mitochondria to cytoplasm, and hence, has an anti-apoptotic effect. Therefore, peptides with ability to localize at the mitochondrial membrane and disrupt the VDAC1-HK-II binding can be studied as specific anticancer agents. In the search of antitumor peptides, Woldetsadik *et al.*[34] have covalently coupled pHK to a short penetration accelerating segment (PAS) to obtain a cell-penetrating peptide pHK-PAS. In HeLa cells, the pHK-PAS has exerted a depolarization effect on the mitochondrial membrane and has inhibited the mitochondrial respiration and glycolysis. Subsequently, Palanikumar *et al.*[37]

synthesized another peptide PAS-pHK, which used to deliver miR-216 considering that the tumor suppressor miRNA is down-regulated in several malignancies. It should be noted that the miR-126 cargo has synergistically enhanced the anti-cancer effect of PAS-pHK. Chiara *et al*.[35] have conjugated a TAT sequence (i.e. HIV-1 protein-derived CPP) at the N-terminal of pHK to obtain the TAT-HK peptide with the purpose to facilitate the pHK entry into HeLa cancer cells. TAT-HK has enabled the detachment of HK-II from mitochondria and thus has activated apoptosis. The dissociation of HK-II from mitochondria has been suggested as a pro-apoptotic stimulus because such a process requires VDAC to open the mitochondrial permeability transition pore (PTP). As a consequence, the integrity of the mitochondrial membrane is lost and proteins (like Cyt-c) are released from mitochondria.

In a previous study, we have reported a new type of mitochondrial targeted peptide, which comprises a covalently conjugated positively-charged sequence pKV (KVLKQRAKKK) to the N-terminal pHK (MIASHLLAYFFTELN) of HK-II, yielding a new amphiphilic CPP (pHK-pKV).[25] To increase the cellular uptake of the pHK-pKV peptide, we further conjugated a hydrophobic palmitic acid (Pal) alkyl chain to the N-terminal of pHK-pKV. The created amphiphilic peptide Pal-pHK-pKV displayed α-helical structure. Depending on the concentration, both pHK-pKV and Pal-pHK-pKV peptides (Figure 1) can form nano-assemblies owing to their amphiphilic nature. Despite that the physico-chemical results have suggested that the amphiphilic modifications may be beneficial for the cell-penetrating properties of the new peptides, the effects of these peptide amphiphiles on the proliferation and apoptosis of human A549 lung cells have not been investigated yet.

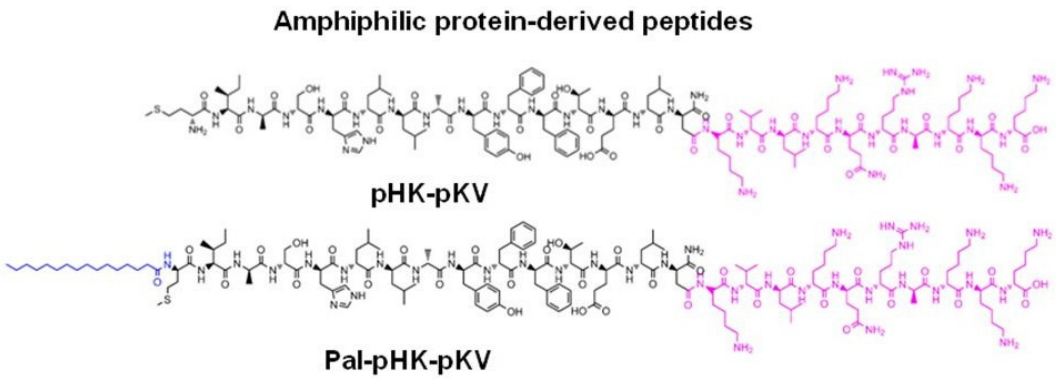

Figure 1. Chemical structures of pHK-pKV and Pal-pHK-pKV.

The purpose of the present study is to examine the effects of the amphiphilic pHK-pKV and Pal-pHK-pKV peptides on the proliferation and apoptosis of human A549 lung cells *in vitro*. In this study, dipalmitoyl phosphatidylglycerole (DPPG) monolayer used as the lipid model membrane to study the interaction of pHK-pKV or Pal-pHK-pKV with cell membrane by using Langmuir-Blodgett technique. The local interaction of peptides with the cellular membrane is then further evidenced by two-photon excitation microscopy employing the dual-fluorescent membrane probe *N,N'*-diphenyl-dihydrodibenzo[*a,c*] phenazine (DPAC) with vibration-induced emission (VIE) property. The biological activity mechanism, resulting from the enhanced cellular uptake of the lipidated peptide, is evaluated using several bioassays probing mitochondrial potential, cell cycle arrest, apoptosis, protein expression, enzymatic activity as well as immunofluorescence.

2. Materials and Methods

2.1. Materials and biochemical reagents

The peptides pHK-pKV (MW 2979.9) and Pal-pHK-pKV (MW 3217.2) were custom synthesized by Nanjing Peptide Biotechnology Co., Ltd. (Nanjing, China) according to a previously established method.[25] Dulbecco's Modified Eagle Medium (DMEM), Fetal

Bovine Serum (FBS) and Penicillin/Streptomycin reagents were purchased from GIBCO (Grand land, NY, USA). 3-(4,5-dimethylthiazol-2-yl)-2,5-diphenyltetrazolium bromide (MTT), 0.25% trypsin-EDTA and dimethyl sulfoxide (DMSO) were purchased from Sigma (St. Louis, MO, USA). Cell cycle detection kit and mitochondrial membrane potential detection kit and Mito Tracker® Deep Red FM were purchased from Shanghai Maokang Biotechnology Co., Ltd (Shanghai, China). The Annexin V-FITC apoptosis detection kit was purchased from Boster Biological Technology Co., Ltd (Shanghai, China). Caspase 3, caspase 8 and caspase 9 colorimetric assay kits were purchased from Nanjing KeyGen Biotech. Co., Ltd (Nanjing, China). Antibodies against Cyclin A1, proliferating cell nuclear antigen (PCNA), the cyclin dependent kinase (CDK 2), p21, caspase 3, caspase 8, caspase 9, β-actin, cytochrome c (Cyt-c), hexokinase HK-II, FITC goat anti-rabbit immunoglobulin G (IgG), HRP goat anti-rabbit immunoglobulin G (IgG) were purchased from ABclonal (Wuhan, China). Other antibodies were purchased from the Proteintech Group Int. (Rosemont, IL, USA). Antifade mounting medium with DAPI was purchased from Dalian Meilun Biology and Technology Co. Ltd. (Dalian, China). The DPAC was a gift from Prof. JianHua Su, School of Chemistry and Molecular Engineering, East China University of Science and Technology.

2.2. Langmuir-Blodgett technique

DPPG was dissolved in a mixed solution of chloroform and methanol with a final phospholipid concentration of 0.8 mg/mL. Adding PBS buffer (0.01 M, pH 7.4, 200 mL) to a clean plastic tank as the subphase to make it evenly distributed, and then hanging the cleaned suspension needle on the detection arm to correct the surface tension of the

subphase solution at 25 °C. 10 μL micro-injector was used to carefully add phospholipid solution (10 μL) to the PBS subphase, and let it stand for 30 min to form a stable monomolecular membrane. Then the pre-prepared peptide solution was added in the PBS subphase liquid surface. Through the real-time monitoring of the KN2002 LB film analyze system (BiolinScientific, Sweden), a surface pressure-time (π-t) isotherms was obtained.

2.3. Cell culture

Human A549 lung carcinoma cells and human bronchial epithelial 16HBE cells were cultured in DMEM medium that was supplemented with 10% (v/v) FBS and 1% (v/v) Penicillin/Streptomycin mixture. Cells were cultivated at 37 °C in a humidified atmosphere of 5% CO_2.

2.4. Cytotoxicity assay

The cytotoxic effects of the peptides pHK-pKV and Pal-pHK-pKV on the cellular viability were assessed using the MTT assay. For cytotoxicity assay, the cells were seeded in 96-well plates (SPL Life Sciences Co. Ltd, Korea) at a density of 5×10^3 cells/well and kept at 37 °C in an atmosphere of 5% CO_2 for 24 h. The peptides were diluted to the desired concentration with DMEM medium. The cells were incubated at increasing concentrations of peptides in the series 0, 3.125, 6.25, 12.5, 25, and 50 μM. The incubation was performed at 37 °C for 24 h. MTT solution (5 mg mL^{-1}) was added (10 μL) to each well and incubated at 37 °C for 4 h. Subsequently, DMSO (100 μL) was added to end the reaction and the absorbance of the product was measured at 570 nm by a Synergy NEO HTS multi-mode microplate reader (Bio Tek, USA). Data were interpreted as the percentage of viable cells compared with that of the controls (non-treated cells).

2.5. Cell membrane local heterogeneity characterization by a membrane bioimaging probe with vibration-induced emission (VIE) properties

The interaction of the amphiphilic peptides with the living A549 lung cells is expected to modify the membrane properties. Cell membrane local properties characterization was done using the DPAC as a cellular membrane bioimaging probe with vibration-induced emission (VIE) properties.[38-41] The excitation of the DPAC transforms the molecular configuration from a bent state to a planar state. The photoinduced bent-to-planar transformation involves out-of-plane bending of the V-shaped polycyclic conjugated structure. The excited-state (ES) planarization of the DPAC moiety produces highly colour-tunable fluorescent images as the emission of DPAC is dependent on the environmental viscosity, polarity, and temperature. The photo-induced bent-to-planar transformation may be hampered in viscous or heterogeneous membrane environment. Thus, bright blue fluorescence may be emitted from the retained saddle-shaped conformation. Depending on the local membrane properties, fluorescence colour-tuning process from orange-red to blue may be observed with the VIE-active DPAC bioimaging probe.

The A549 cells (5×10^4 cells per mL) were seeded into 35 mm glass bottom dish and then were incubated with pHK-pKV (6.25 μM) or Pal-pHK-pKV (6.25 μM) peptides for 24h. After washing once with PBS, fresh DMEM medium containing the DPAC dye (20 μM) was then incubated with the cells for 10 min. A two-photon excitation TCS SP8 DIVE (Deep In Vivo Explorer) microscopy system with spectrally tunable detection (Leica, Germany) was used to continuously scan the full emission spectrum (380-770 nm) for 10 min, the excitation wavelength was set at 340 nm.

2.6. Cell cycle analysis

The cell cycle analysis was performed by DNA staining with propidium iodide (PI). In brief, the A549 cells were seeded into 6-well plates (SPL Life Sciences Co. Ltd, Korea) at a density of 1×10^5 cells per mL and kept at 37 °C in an atmosphere of 5% CO_2 for 24 h. The two peptides were then added at concentrations 6.25 μM and 25 μM into the wells and incubated for 24 h. After incubation, adherent and floating cells were all collected by centrifugation and washed by PBS, then fixed in ethanol (75% in PBS). The fixed cells were kept at 4 °C overnight. Then, they were washed with PBS and stained with PI staining solution, which contained staining buffer (0.4 mL per sample), 25×PI (15 μL per sample), and 100×RNase A (4 μL per sample) at 37 °C for 30 min in the dark. The excitation wavelength was 488 nm, and the fluorescence emission maximum was at 585 nm. The fluorescence of PI-stained cells was determined by the CytoFLEX LX Flow cytometer (Beckman Coulter, Inc., Brea, CA, USA). The percentages of the cells in the G1, S, and G2/M phases were determined using the software Flowjo 7.6 (Tree Star, Ashland, OR, USA).

2.7. Cell apoptosis assay

Cell apoptosis was measured using the Annexin V-FITC apoptosis detection kit. In practice, A549 cells were seeded into 6-well plates at density 1×10^5 cells per mL and were incubated for 4 h at 37 °C. Afterwards, the cells were treated with varying peptides doses for 4 h. After peptide incubation, the cells were washed twice with cold PBS and were collected by centrifugation. The cell suspensions were incubated with binding buffer (300 μL) and Annexin V-FITC (10 μL) for 20 min as well as PI (1 μL) for 10 min at room

temperature in the dark. The fluorescence of the peptide-treated cells was measured by the CytoFLEX LX Flow cytometer. The data were analyzed with the CytExpert software. The FITC-conjugated Annexin V and the PI dye were excited at wavelength 488 nm. The emissions were recorded at wavelengths 525 nm and 585 nm for the FITC-conjugated Annexin V and PI, respectively.

2.8. Mitochondrial membrane potential assay

Depolarization of mitochondrial membrane potential ($\Delta\Psi_m$) was detected using the fluorescent probe JC-1 (cyanine dye). In practice, cells were seeded into glass bottom dishes with diameter 20 mm (In Vitro Scientific, USA) at density 1×10^4 cells per mL overnight and were treated with the studied peptides at increasing concentrations (3.125 μM, 6.25 μM and 25 μM) for 4 h. Each dish was incubated with JC-1 staining solution and staining buffer according to the protocol of the supplier. Then, the cells were washed once with cold PBS. A new culture medium containing JC-1 (0.5 mL) staining reagent was added at 37 °C for 20 min in the dark. After incubation, the supernatant was aspirated and the cells were washed twice with JC-1 staining buffer. Fresh DMEM was added into the dishes after washing. The JC-1 monomeric or aggregated forms were detected using Zeiss LSM 710 laser scanning confocal microscope (Zeiss, Oberkochen, Germany). Dye excitation was performed at 488 nm (green) in order to detect fluorescence emission at 522 nm (green) of the monomeric JC-1. An excitation wavelength of 561 nm (red) was used to detect the fluorescence of JC-1 aggregates with a maximum at 632 nm (red).

2.9. Caspase catalytic activities assay

The catalytic activities of caspase 3, caspase 8 and caspase 9 were determined by caspase colorimetric assay kits. Briefly, A549 cells were treated with pHK-pKV (6.25 and 25 μM) or Pal-pHK-pKV (6.25 and 25 μM) for 24 h in 10 cm dishes. After that, the cells were washed with PBS twice, re-suspended in lysis buffer (100 μL), and incubated on ice for 30 min. The cells were pelleted by centrifugation at 10000 rpm for 1 min at 4 °C and separated from the supernatant. Then, the concentration of protein in the total cell lysates was measured using the BCA protein quantification kit (Epizyme Biotech, Shanghai, China). Subsequently, cell lysates were incubated with 2× reaction buffer (50 μL) and caspase substrate (5 μL) at 37 °C for 4 h in dark. The absorbance of the samples was measured at 405 nm using a microplate reader.

2.10. Western Blot

The cell protein was extracted by a commercial column tissue and cell protein extraction kit (Epizyme Biotech, Shanghai, China). After incubation with pHK-pKV (6.25 and 25 μM) or Pal-pHK-pKV (6.25 and 25 μM) for 24 h, the cells were washed with cold PBS twice, and the supernatant was aspirated. Then, a lysis buffer was added to the samples (the volume ratio of protease inhibitor to cell lysis buffer was 1:100). The cell lysates were collected into pre-cooled purification tubes and centrifuged at 4 °C for 30 s at 14000 rpm.

The protein concentration was measured by the BCA protein quantification kit with bovine serum albumin (BSA) as a standard. After adding the running buffer, the proteins were separated on 15-well Hepes-Tris Gel (Epizyme Biotech, Shanghai, China). The proteins were transferred to 0.45 μm polyvinylidene difluoride membrane (PVDF) (Merck Millipore, Billerica, MA, USA) in tris-glycine buffer, and then blocked with 1× protein free

rapid blocking buffer (10 mL) (Epizyme Biotech, Shanghai, China) for 30 min. After that, the membrane was incubated overnight with rabbit anti-human anti-bodies at 4 °C, washed 4 times, and then exposed to HRP goat anti-rabbit IgG (H+L) for 30 min, and washed again for four times. Afterwards, each sample was visualized by Omni-ECL™ Femto light chemiluminescence kit (Epizyme Biotech, Shanghai, China) and ChemiDoc™ MP imaging system (BioRad Laboratories, Hercules, CA, USA).

2.11. Immunofluorescence staining

The A549 cells were seeded into 35 mm glass bottom dish at a density of 5×10^4 cell per mL and incubated for 24 h. Then, the cells were treated with pHK-pKV (25 μM) and Pal-pHK-pKV (6.25 μM), respectively, for 12 h at 37 °C. After incubation, the cells were washed with PBS, fixed with 4% paraformaldehyde for 10 min, and permeabilized with 3% bovine serum albumin-containing 0.1% Triton X-100 for 30 min. Then, HK-II polyclonal antibody and Cyt-c polyclonal antibody were added at a 1:200 dilution, and the cells were incubated for 2 h. FITC-goat anti-rabbit IgG was then added at a 1:200 dilution and the cells were incubated for 30 min. Finally, the cells were stained with a mitochondrial dye (1 mM) and an appropriate amount of antifade mounting medium with DAPI was put on. The cells were imaged using Zeiss LSM 710 laser scanning confocal microscope.

2.12. Statistical analysis

All experiments were repeated at least three times. Statistical analysis was performed using GraphPad Prism 8.0 software (GraphPad Software, La Jolla, CA, USA). Statistical significance between every two experimental groups was assessed by unpaired Student's t test. A value of $p > 0.05$ was considered as non-significant.

3. Results and Discussion

3.1. The interaction of pHK-pKV and Pal-pHK-pKV with lipid membrane interfaces

VDAC1 is overexpressed in many cancer types including human non-small cell lung cancer. In our previous study, we found that the mitochondria-specific synthetic peptide amphiphiles pHK-pKV and Pal-pHK-pKV (Figure 1), derived by engineering of the 15 amino acid terminal fragments of the hexokinase-II protein, are able to locate to mitochondria and trigger mitochondria-mediated A549 cancer cell apoptosis, while Pal-pHK-pKV has an enhanced bioactivity in terms of cell cancer cytotoxicity, the degree of cellular uptake, and mitochondrial localization.[25] From the physicochemical properties of pHK-pKV and Pal-pHK-pKV, both of them can self-assemble into ellipsoid-like aggregates with nanometric dimensions.[25] The secondary structures of pHK-pKV and Pal-pHK-pKV involved partial α-helical conformations. Pal-pHK-pKV is characterized by a higher helicity, which suggests a superior affinity for interaction with lipid membranes.

In order to examine the effects of the amphiphilic pHK-pKV and Pal-pHK-pKV peptides on the proliferation and apoptosis of human A549 lung cells *in vitro*, the interaction with the cellular model membrane is evidenced by using Langmuir-Blodgett technique.[42, 43] Phospholipid molecules (DPPG) with negatively charge formed monolayers was used to simulate cell membranes to explore the interaction between pHK-pKV or Pal-pHK-pKV and cell membranes. The π-t isotherms can reflect the dynamic interaction of pHK-pKV and Pal-pHK-pKV with DPPG monolayers. As shown in Figure 2, pHK-pKV solution was added at the initial surface pressure (π_{ini}) of 15 mN m^{-1}. After the addition of pHK-pKV, the surface pressure of the model lipid membrane first rose rapidly, and then

reached a plateau. The positively charged cationic peptide pKV can interact electrostatically with the negatively charged DPPG. And also, there is the hydrophobic interaction between DPPG and pHK-pKV. Thus, pHK-pKV and DPPG can form a mixed membrane, and the surface pressure gradually reaches a saturated and stable state. At around 1250 s, the surface pressure has a slight upward trend within the measuring time, indicating that there are new pHK-pKV molecules adsorbed to the interface, combined, expanded and rearranged.[44]

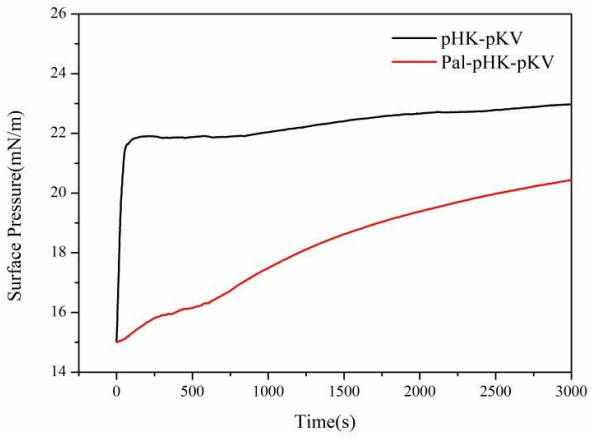

Figure 2. Time dependence of the surface pressure changes during the interaction of pHK-pKV and Pal-pHK-pKV with DPPG monolayer.

From Figure 2, it can be found that the surface pressure increased gently within the measuring time, which was due to the strong interaction between Pal-pHK-pKV and DPPG. Compared with pHK-pKV, Pal-pHK-pKV becomes more hydrophobic due to the hydrophobic palmitic (Pal) alkyl chain. So, the hydrophobic interaction between Pal-pHK-pKV molecules resulting in a smaller effect on the surface pressure of the phospholipid membrane at the initial stage of the addition of Pal-pHK-pKV. And then, the surface pressure has a moderate upward trend within the measuring time, indicating that there are more Pal-pHK-pKV molecules adsorbed to the interface, combined, expanded and

rearranged. Moreover, the Δπ (the difference between the final surface pressure and the initial surface pressure) of Pal-pHK-pKV was smaller than that of pHK-pKV (Figure 2), which suggested that the DPPG and Pal-pHK-pKV formed the more orderly arrangement due to the hydrophobic and electrostatic interaction between Pal-pHK-pKV and DPPG molecules.[45] This result is consistent with the higher helicity of Pal-pHK-pKV, which suggests a superior affinity for interaction with lipid membranes.

3.2. pHK-pKV and Pal-pHK-pKV peptides selectively inhibit the proliferation of human A549 cells versus 16HBE cells

We compared the cytotoxicity of pHK-pKV and Pal-pHK-pKV to two human cell lines, A549 and 16HBE, which were treated with 3.125, 6.25, 12.5, 25 and 50 μM pHK-pKV or Pal-pHK-pKV, respectively for 24 h. In the employed MTT test, MTT is reduced by the mitochondrial enzyme succinate dehydrogenase in the living cells to blue-purple crystal formazan, while no effect is detected with dead cells.[46] The measured changes of the absorbance in DMSO solvent reflect the impact on the cellular viability.[47] Figure 3 showed the determined concentration-dependent decrease in cellular viability. It evidenced that Pal-pHK-pKV has a stronger anti-tumor effect than pHK-pKV. This is attributed to the hydrophobic palmitic acid chain of the lipidated Pal-pHK-pKV molecule. The hydrophobic modification appears to promote the anti-tumor properties of the peptide.

The half maximal inhibitory concentrations (IC_{50}),[48] determined for the human A549 lung cancer cells, were IC_{50} of 21.5±0.32 μM and 6.5±0.14 μM for the pHK-pKV and Pal-pHK-pKV peptides, respectively. Interestingly, the two peptides displayed a cytotoxic selectivity and were less toxic to human 16HBE epithelial cells, shown in Figure S1.

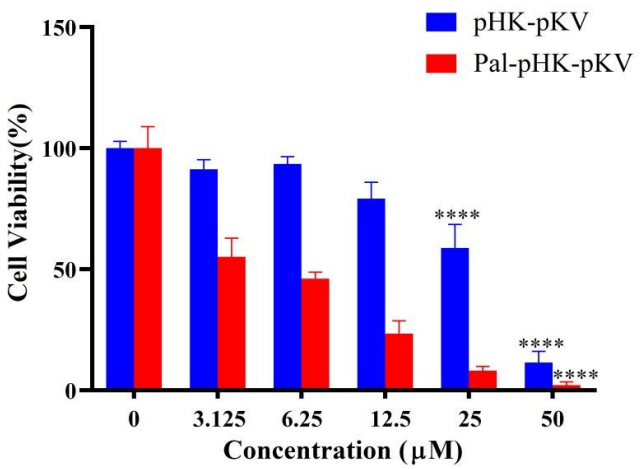

Figure 3. Effects of pHK-pKV and Pal-pHK-pKV peptides on cellular viability. Human A549 cells were incubated with pHK-pKV or Pal-pHK-pKV peptides, respectively for 24 h in concentration series. Cell viability was determined using the MTT assay. Untreated cells were taken as control. ****$p<0.0001$ compared to control. Data were presented as mean ± S.D. (n=5).

3.3. Lipidation by palmitic chains enhances the peptide interaction with membranes and cellular uptake

We also evaluated the interaction between the designed peptides and the A549 cell membranes using a dual-fluorescent bioimaging probe DPAC. The DPAC is a typical dye with vibration-induced emission (VIE) properties.[38-40] In the excited state (ES), the large "red shift" in the emission (emission spectrum shift to higher wavelengths) originates from ES planarization. At variance, a "blue shift" (emission spectrum shift to lower wavelengths) is observed when the ES planarization is hindered by the membrane environment.[40]

The bioimaging results with DPAC are presented in Figure 4(a) and the fluorescence intensities are analyzed in Figures 4(b, c). The microdomains refer to the areas with relatively strong fluorescence intensity, in which the peptides interact with the A549 cell

membrane. The flat region in Figure 4(b, c) refers to the area with relatively weak fluorescence intensity, where the peptide-cell membrane interactions were weak. The results show a blue shift of the DPAC fluorescence maximum emission wavelength when comparing DPAC-labeled A549 cell membranes treated with pHK-pKV and Pal-pHK-pKV, respectively (from 475 nm in Figure 4(b) to 462 nm in Figure 4(c)). This indicates that the cell penetrating capacity of the lipidated Pal-pHK-pKV peptide with a hydrophobic Pal chain is higher than that of the unmodified peptide (pHK-pKV). The membrane environment for the DPAC probe becomes more hydrophobic upon insertion of the Pal chains into the cellular membrane. The obtained images reveal that the distribution of the Pal-pHK-pKV peptide in the membrane surrounding is heterogeneous. Therefore, it may be suggested that the increased apoptotic effect of Pal-pHK-pKV (as compared to that of the pHK-pKV peptide) may be due to formation of microdomains or pores resulting from clustering of the Pal hydrophobic moieties. This correlates with the observed blue shift of the DPAC emission spectrum (i.e. hindered excited-state planarization under the conditions of local cell membrane heterogeneity). The above results are consistent with the results of Langmuir-Blodgett Film experiment and the cytotoxicity experiment of pHK-pKV and Pal-pHK-pKV to A549 cell line.

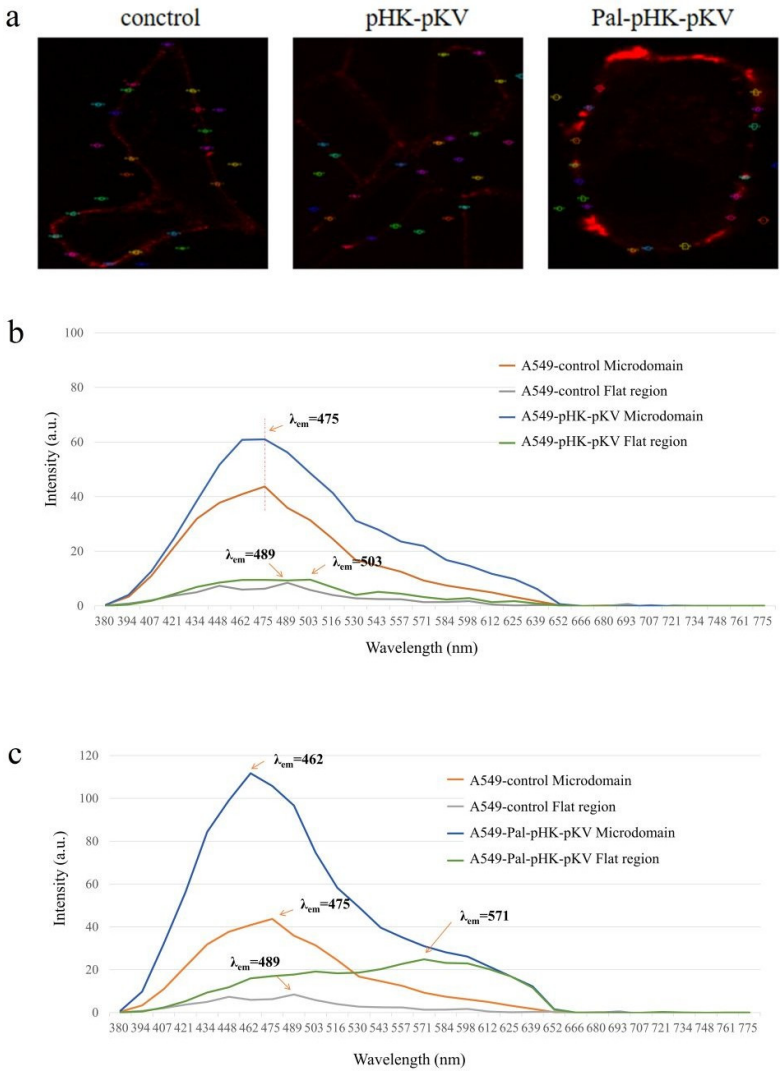

Figure 4. (a) Bioimaging of A549 lung cell membranes in the absence or presence of peptide treatment for 24h based on labeling interaction with the DPAC: Control (left image), 6.25 μM pHK-PKV and 6.25 μM Pal-pHK-pKV (right image); Fluorescence emission spectra of the DPAC probe deduced in different regions of the A549 cells membrane incubated with (b) pHK-pKV at 6.25 μM and (c) Pal-pHK-pKV at 6.25 μM for 24 h.

3.4. pHK-pKV and Pal-pHK-pKV peptide-induced cell cycle arrest in the S phase and apoptosis detection in human A549 cells

The effects of the amphiphilic peptides on the cell cycle arrest and apoptosis of A549 cells were further examined by flow cytometry using PI staining (Figure 5) or Annexin/PI staining (Figure S2), respectively. After 24 h incubation with the peptides pHK-pKV or Pal-pHK-pKV, the intracellular DNA content changed accordingly. The number of cells in the G1 phase gradually decreased with the increase of the peptide concentration, whereas the number of cells in S phase increased (Figure 5(a)). Both peptides arrested the cell cycle in the S phase and prevented the progression to the G2/M phase. Thus, the proliferation of the A549 cells was blocked at mitosis. It should be emphasized that the lipidated peptide Pal-pHK-pKV exerted more significant arrest effect on the cell cycle than that of pHK-pKV when incubated with the A549 cells at same concentration.

Cell cycle arrest is regarded relevant to apoptosis. The proliferating cell nuclear antigen (PCNA) is a key factor in the S phase, which depends on the expression of cyclin A1 and cyclin dependent kinase (CDK 2) (see Figure 8 below).[49] In addition, it is related to the activity of p21.[50] Both down-regulation of the cell cycle regulatory complex (cyclin A1/CDK 2/PCNA) and up-regulation of p21 expression contribute to S-phase arrest.

Results of cell apoptosis measurements with the Annexin/PI kit were presented in Figure S2. For cells treatment with 6.25 μM pHK-pKV and Pal-pHK-pKV, the apoptotic rates (Annexin V+/PI- and Annexin V+/PI+) were determined to be 5.03% and 78.19%, respectively. This suggests that both peptides can induce A549 cellular apoptosis.

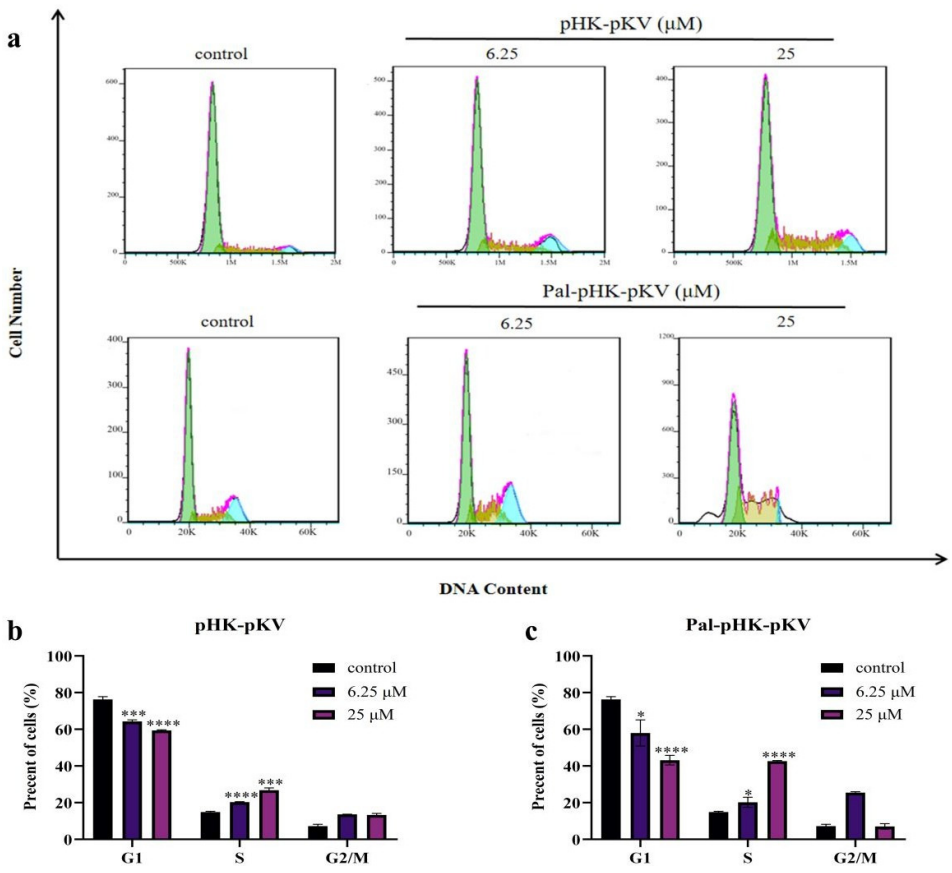

Figure 5. Cell cycle flow cytometry assay with A549 cells. (a) Cell cycle distribution upon A549 cells incubation with pHK-pKV and Pal-pHK-pKV at increasing peptide concentrations. Green represents the G1 phase, brown represents the S phase, and blue represents the G2/M phase. Histograms show quantitative results about cell cycle distribution upon treatment with (b) pHK-pKV or (c) Pal-pHK-pKV peptides. Untreated cells were taken as control. *p<0.05, ***p<0.001, ****p<0.0001 compared to control. Data were presented as mean ± S.D. (n=3).

3.5. pHK-pKV and Pal-pHK-pKV peptide-induced mitochondrial-dependent apoptosis in A549 cells revealed by changes in the mitochondrial membrane potential

Mitochondrial dysfunction in pHK-pKV and Pal-pHK-pKV peptide-treated A549 cells was determined by the changes in the mitochondrial membrane potential $\Delta\Psi_m$ (Figure 6). A cationic cyanine dye, JC-1[51], was used to detect the changes, $\Delta\Psi_m$, associated with potential-dependent dye accumulation in mitochondria. In healthy mitochondria, the JC-1 dye aggregates in the mitochondrial matrix in the form of aggregate assemblies, which display a strong fluorescence emission at 632 nm (shown in red in Figure 6). Due to the membrane interaction with the cell-penetrating peptides, the mitochondrial membrane potential can decrease or even become negligibly small. The JC-1 dye predominantly exists in a monomeric form in the cytoplasm, where it displays fluorescence emission at 522 nm (shown in green in Figure 6).[52-54]

Figure 6 revealed that the JC-1 fluorescence in A549 cells gradually changes from red to green after pHK-pKV and Pal-pHK-pKV peptide incubation for 4 h. These results indicated the decrease of the mitochondrial membrane potential in the peptide-treated A549 cells. Moreover, the data obtained at varying peptide concentrations showed that the mitochondrial membrane potential changes, $\Delta\Psi_m$, were concentration dependent (Figure 6).

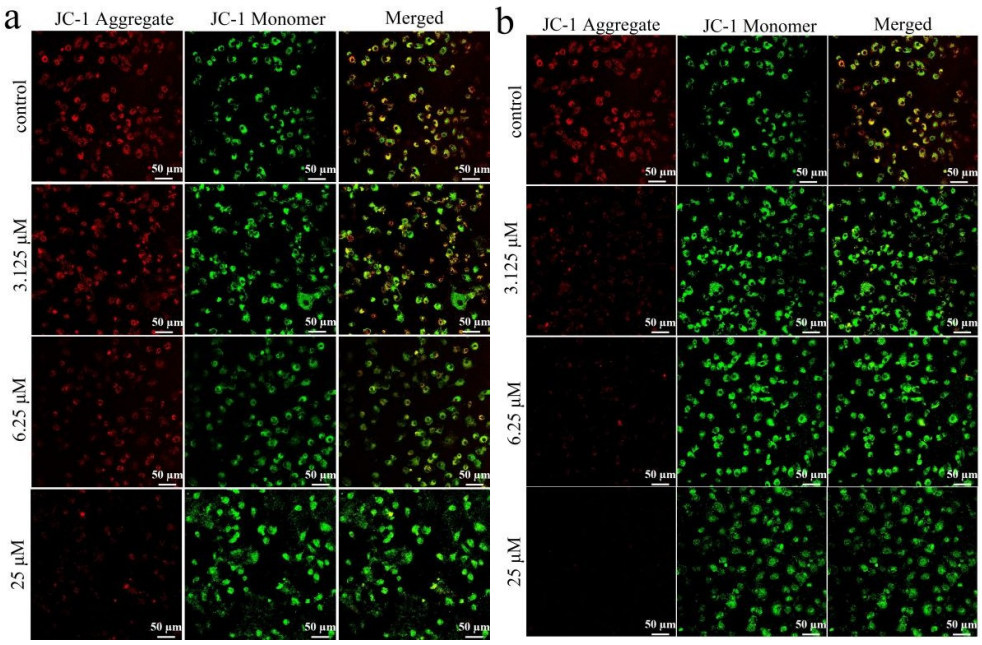

Figure 6. Evaluation of the changes in the mitochondrial membrane potential in A549 cells upon peptide treatment at varying concentrations (3.125 μM, 6.25 μM and 25 μM). Confocal micrographs of JC-1-labeled A549 cells after treatment with (a) pHK-pKV and (b) Pal-pHK-pKV peptide, respectively for 4 h. The domination of the red fluorescence reflects the presence of the aggregated form of the JC-1 dye (healthy mitochondria in non-apoptotic cells), whereas the green fluorescence of the monomeric JC-1 dye reflects the collapse of $\Delta\Psi_m$ leading to cell apoptosis. Scale bars: 50 μm.

3.6. pHK-pKV and Pal-pHK-pKV peptide-activated caspase 3, caspase 8 and caspase 9 in A549 cells

The caspase protein family belongs to cysteine proteases, which plays a key role in cell apoptosis.[55] Once caspase are activated, serial cascade reactions are triggered that may lead to irreversible apoptosis.[56] Among them, caspase 8 is associated with exogenous apoptosis. Caspase 8 can be activated when the death ligand binds to the death receptor. Consecutively, it activates downstream caspase such as caspase 3, caspase 6 and caspase 7, which

ultimately initiate apoptosis.[22, 30] In contrast, caspase 9 is associated with the endogenous mitochondrial pathway. Similar to the role of caspase 8 in the exogenous pathway, caspase 9 can initiate downstream cascades.

Figure 7 showed the concentration-dependent effects of the peptides pHK-pKV and Pal-pHK-pKV on the caspase 8, caspase 9, and caspase 3 activities in human A549 cells. The obtained results indicate that the activities of both caspases in the peptide-treated cells increase significantly in comparison with that in the non-treated control sample. The observed effects are dependent on the peptide concentration. The higher the peptide concentration, the higher are the activities of caspase.

Moreover, the caspase activity for A549 cells incubated with Pal-pHK-pKV peptide appears to be higher than that for incubation with pHK-pKV as same concentration (Figure 7). Overall, it can be concluded that pHK-pKV and Pal-pHK-pKV are not only involved in the mitochondrial pathway of apoptosis, but also have impact on the exogenous apoptosis. This may be due to their cell-penetrating properties.

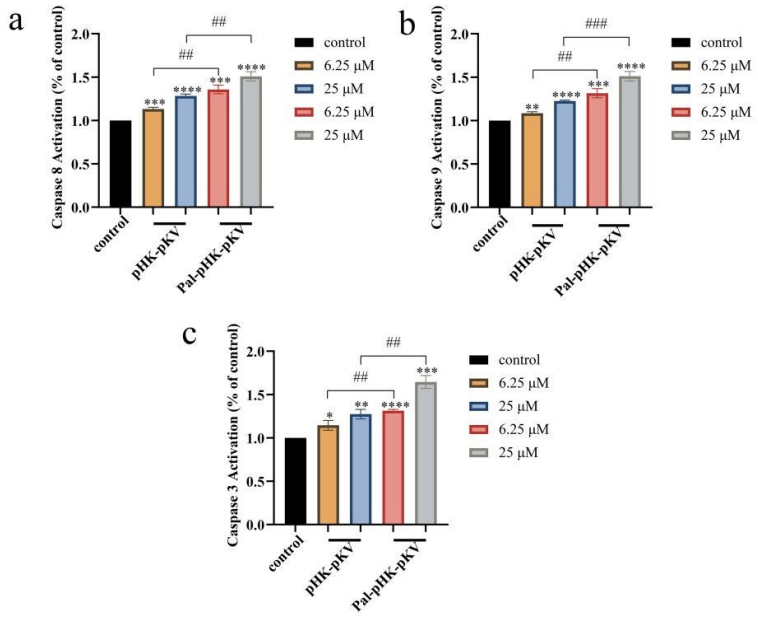

Figure 7. Effects of the pHK-pKV and Pal-pHK-pKV peptides on (a) caspase 8, (b) caspase 9 and (c) caspase 3 activities in human A549 cells. Untreated cells were measured as control. *p<0.05, **p<0.01, ***p<0.001, ****p<0.0001 compared to control. ##p<0.01, ###p<0.001 compared to pHK-pKV. Data were presented as mean ± S.D. (n=3).

3.7. pHK-pKV and Pal-pHK-pKV peptide-induced changes in the expression levels of apoptosis-related proteins

Western blot analysis was performed to characterize the S-phase arrest related protein (cyclin A1/CDK 2/PCNA and p12) expression in A549 cells.[57] Figure 8 showed that 24 h peptide treatment of A549 cells results in decreased expression of cyclin A1, CDK 2 and PCNA and increased expression of p12 as compared to control. This confirmed that both pHK-pKV and Pal-pHK-pKV peptides can arrest the A549 cells in the S phase with more significant blocking effect in the Pal-pHK-pKV treatment group.

On the other hand, Bcl-2 family proteins, Cyt-c and caspases were considered as cell apoptosis-related biomarkers.[58] The obtained results revealed an increased expression of

Bax in the peptide-treated A549 cells. In parallel, a significant decrease of Bcl-2 expression was observed. The expression levels of cleaved caspase 3, 8 and 9 were significantly up-regulated in comparison to the control (Figure 8).

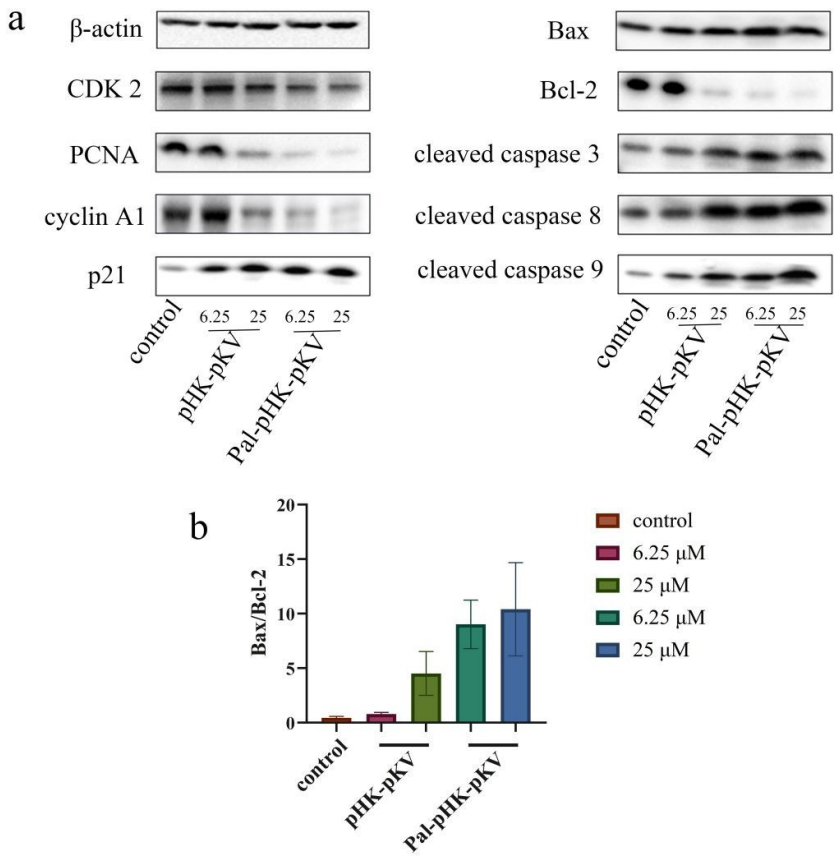

Figure 8. (a) Western blot analysis of proteins involved in the apoptosis process after treatment of A549 cells with pHK-pKV and Pal-pHK-pKV peptides for 24 h in a concentration series. The extracted total cell proteins were immunoblotted with antibodies to characterize the expression of cyclin dependent kinase 2 (CDK 2), proliferating cell nuclear antigen (PCNA), cyclin A1, p12, Bax, Bcl-2, cleaved caspase 3, 8 and 9. (b) Relative Bax/Bcl-2 protein concentrations in peptide-treated A549 cells. Data were presented as mean ± S.D. (n=3).

3.8. pHK-pKV and Pal-pHK-pKV peptides displace the full-length HK-II protein from the mitochondrial membrane and generate the release of cytochrome c

Our study verified the hypothesis whether modified pHK fragments can replace the over-expressed endogenous HK-II[34], thereby blocking the interaction between HK-II and VDAC1 and triggering the release of Cyt-c that ultimately leads to cell apoptosis. We assume that this is valid for the peptides pHK-pKV and Pal-pHK-pKV.

Immunofluorescence colocalization was used to determine the changes in the location of HK-II and Cyt-c in the human A549 lung cells. The orange fluorescence spots in Figure 9 reveal that the red fluorescence from mitochondria is co-localized with the green fluorescence from the HK-II or Cyt-c proteins in the control group without peptide treatment. Such orange fluorescence was rarely observed with A549 cells treated with pHK-pKV and Pal-pHK-pKV peptides. This indicates that the HK-II protein was replaced by the amphiphilic peptide fragments, and thus dissociated from mitochondria. It can be concluded that Cyt-c was released from mitochondria into the cytoplasm after cell treatment with pHK-pKV and Pal-pHK-pKV peptides.

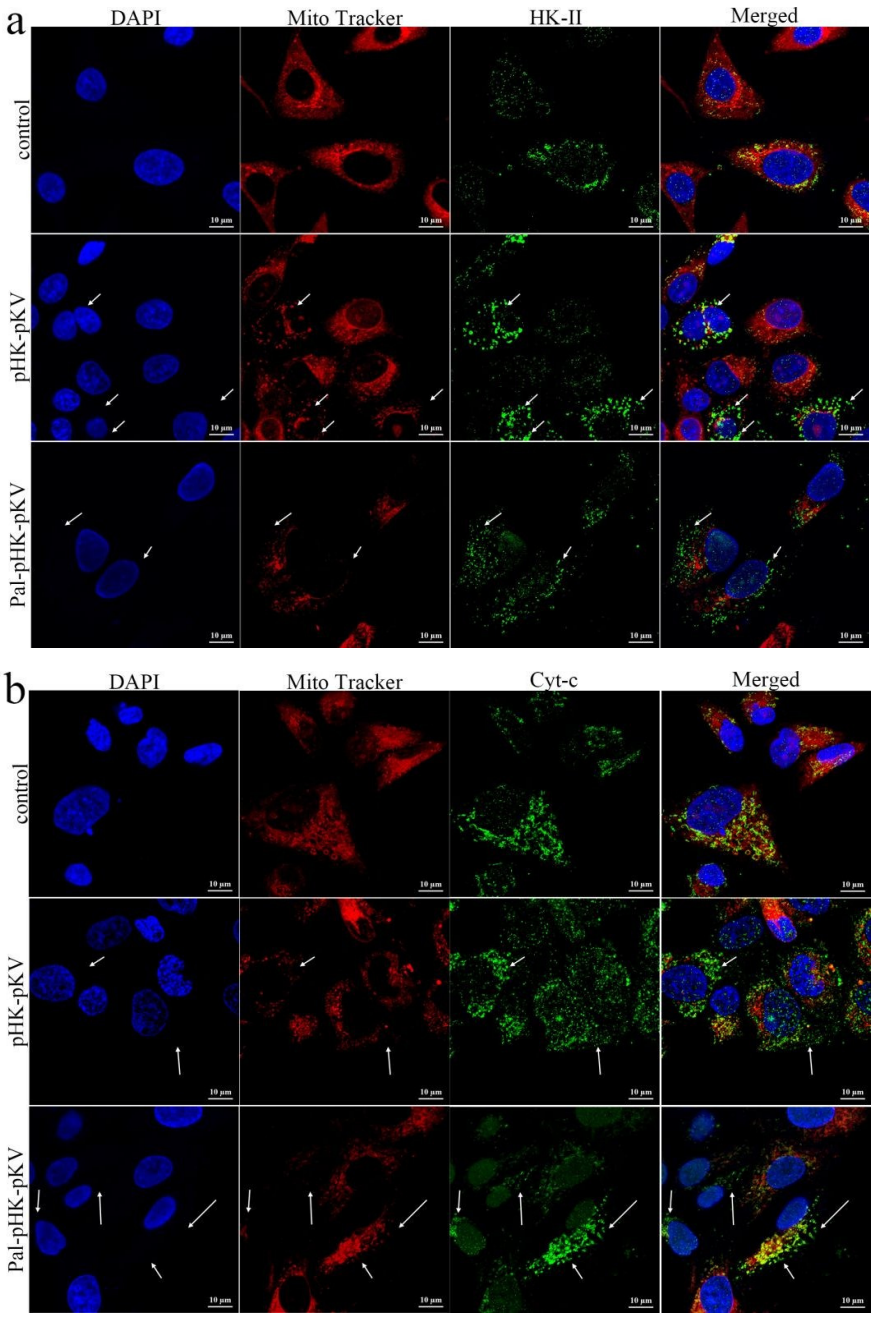

Figure 9. Intracellular distribution of (a) HK-II and (b) Cyt-c proteins probed by confocal laser scanning microscopy (CLSM) imaging. The blue fluorescence marks the cell nucleus, red fluorescence indicates mitochondria, and green fluorescence indicates the target proteins HK-II or Cyt-c stained for immunofluorescence detection. Scale bars: 10 μm.

Figure 10 summarizes the pathway of the biological activity of the pHK-pKV and Pal-pHK-pKV peptides in induction of apoptosis in human A549 lung cells. Our attention focused on the endogenous mitochondrial pathway, in which the peptides provoke depolarization of the mitochondrial membrane potential, related DNA damages (cell cycle arrest), activated expression of pro-apoptotic proteins such as Bax, and decreased expression of Bcl-2 and other anti-apoptotic proteins. Once Cyt-c is released, which activates caspase 9, and then activates caspase 3, cell apoptosis is triggered. This leads to A549 cell death.

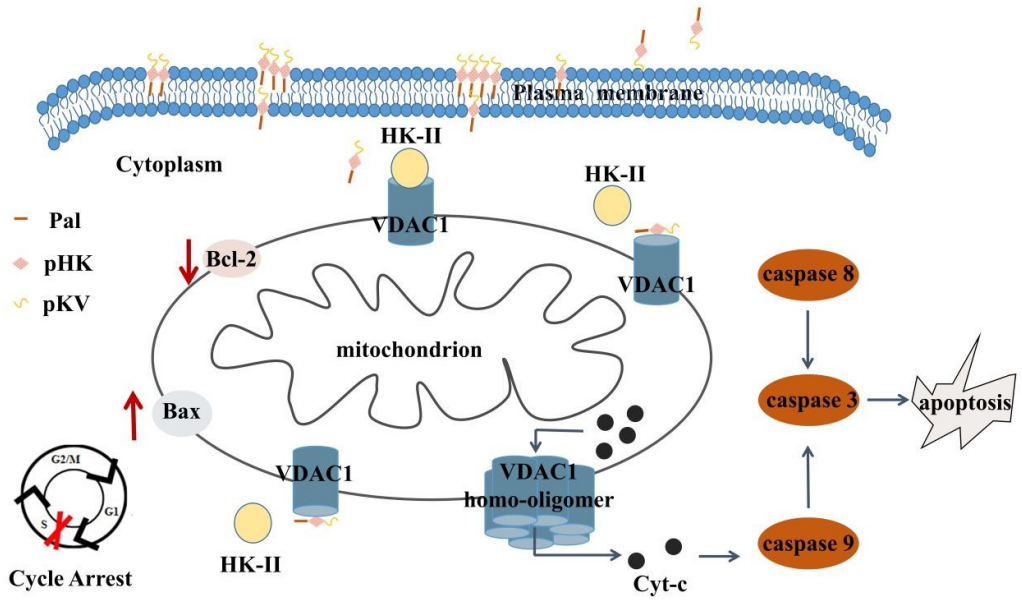

Figure 10. Mechanism of Pal-pHK-pKV and pHK-pKV biological activity in human lung carcinoma A549 cells. The lipidated cell-penetration peptide Pal-pHK-pKV enters the cytosol and targets the membrane protein VDAC1. The displacement of the endogenous full-length HK-II weakens the VDAC1-HK-II interaction. The lipidated Pal-pHK-pKV causes S phase arrest of the cell cycle, which leads to depolarization of the mitochondrial membrane $\Delta\Psi_m$, release of Cyt-c, and finally apoptosis.

4. Conclusion

In conclusion, the present work elucidated the biological mechanism of pHK-pKV and Pal-pHK-pKV induced apoptosis in human A549 lung cells (Figure 10). After binding to mitochondria, both pHK-pKV and Pal-pHK-pKV replaced the endogenous full-length HK-II protein and diminished the VDAC1-HK-II interaction at the mitochondrial membrane. In cancer cells, the peptides caused depolarization of the mitochondrial membrane potential, up-regulation of the Bax expression, down-regulation the Bcl-2 expression, and increase of the enzymatic activities of caspase 9 and caspase 3, thus inducing mitochondria-mediated apoptosis in A549 cells. The two peptides also activated the enzymatic activity of caspase 8, indicating that the pathway of exogenous apoptosis is also involved in the overall biological mechanism. It is worth noting that pHK-pKV and Pal-pHK-pKV are much less toxic to non-cancerous 16HBE cells, which implies that the designed peptides have selective cytotoxicity.

For cancer cells, the lipidated peptide Pal-pHK-pKV exhibited stronger interaction with the membrane as compared to pHK-pKV, which was demonstrated by Langmuir-Blodgett technique and two-photon excitation microscopy. Thus, the enhanced uptake of Pal-pHK-pKV as a cell-penetrating peptide is characterized. It also provides data support for the dual-fluorescent DPAC to better become a fluorescent probe for biological membranes. Pal-pHK-pKV show potential for the development of a useful anti-cancer therapeutic strategy. The anti-tumor activity fragment pHK is not easily taken up by A549 cells, so the successful delivery of pHK into cells is the main purpose. In addition to structural modification of pHK, it can also be loaded by liposomes, polymer micelles and other drug

carriers to achieve the purpose of delivering anti-tumor active fragments to cells. The synthesis of nanostructured lipid carrier with high biocompatibility to encapsulate pHK may be the next work that can be studied.

Supporting Information

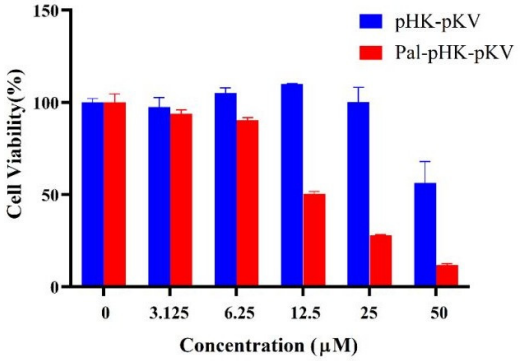

Figure S1. Effect of peptides on cell viability. 16HBE cells were incubated with pHK-pKV or Pal-pHK-pKV respectively for 24 h at concentration series. Cell viability was determined using MTT assay. Untreated cells were taken as control. Data were presented as mean ± S.D. (n=4).

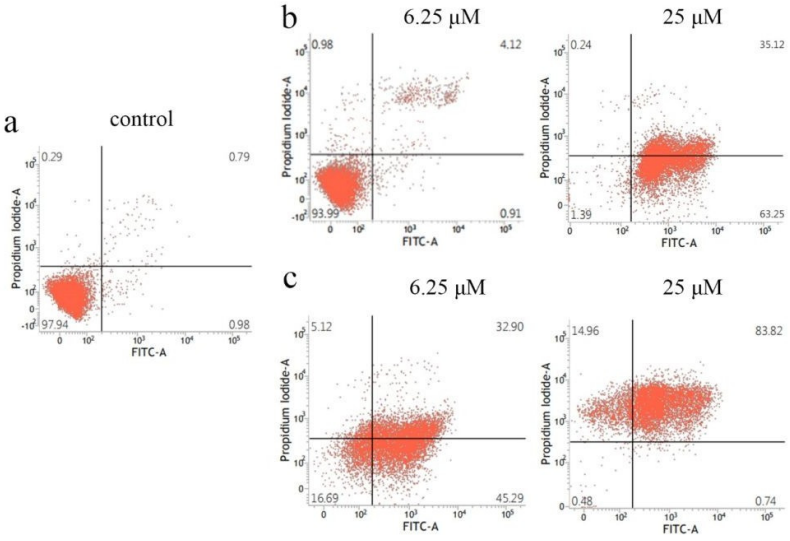

Figure S2. Annexin V/propidium iodide staining of A549 cells treated with (a) pHK-pKV

and (b) Pal-pHK-pKV for 4 h and assessed by flow cytometry.

Declaration of Interest

The authors declare that they have no known competing financial interests or personal relationships that could have appeared to influence the work reported in this paper.

Acknowledgement

This work was supported by the National Natural Science Foundation of China [no. 21872051 and 21573070]. And A.A. acknowledges a membership in CNRS GDR2088 BIOMIM research network.

We thank Dr. Shuyang Tu from Shanghai Advanced Research Institute for helping with the experiment of cell membrane local heterogeneity characterization, Prof. Ling Yang from Fudan University for helping with the analysis of immunofluorescence co-localization and Western Blot results and and Prof. Jianhua Su from East China University of Science and Technology for providing DPAC.

References

[1] Giustini N.P., Jeong A.R., Buturla J., Bazhenova L. Advances in Treatment of Locally Advanced or Metastatic Non–Small Cell Lung Cancer: Targeted Therapy. *Clin. Chest Med*. **2020**, *41*, 223-235.

[2] Karuppasamy, R.; Veerappapillai, S.; Maiti, S.; Shin, W-H.; Kihara, D. Current Progress and Future Perspectives of Polypharmacology: From the View of Non-small Cell Lung Cancer. *Semin. Cancer. Biol*. **2021**, *68*, 84-91.

[3] Masaoutis, C.; Mihailidou, C.; Tsourouflis, G.; Tsourouflis, S. Exosomes in Lung Cancer Diagnosis and Treatment. From the Translating Research into Future Clinical

Practice. *Biochimie*. **2018**, *151*, 27-36.

[4] Tian, H.Q.; Zhang, Y.; Zhang, Q.Y; Li, S.X.; Liu, Y; Han, X.Z. Effects of BENC-511, a Novel PI3K Inhibitor, on the Proliferation and Apoptosis of A549 Human Lung Adenocarcinoma Cells. *BioSci. Trends*. **2019**, *13*(1), 40-48.

[5] Ashiku, S.; DeCamp, M.M. Parenchymal-Sparing Procedures in Lung Cancer: Sleeve Resection of the Lung for Proximal Lesions. *Operative Techniques in Thoracic and Cardiovascular Surgery*. **2006**, *11*(4), 295-309.

[6] Aerts, H.J.W.L.; Bussink, J.; Oyen, W.J.G.; Elmpt, W.; Folgering, A.M.; Emans, D.; Velders, M.; Lambin, P.; Ruysscher, D.D. Identification of Residual Metabolic-active Areas within NSCLC Tumors Using a Pre-radiotherapy FDG-PET-CT Scan: a Prospective Validation. *Lung Cancer*. **2012**, *75*(1), 73-76.

[7] Ashrafizadeh, M.; Zarrabi, A.; Hashemi, K.; Hushmandi, K.; Moghadam, E.R.; Owrang, M.; Hashemi, F.; Makvandi, P.; Goharrizi, M.A.S.; Khan, H. Lung Cancer Cells and Their Sensitivity/resistance to Cisplatin Chemotherapy: Role of MicroRNAs and Upstream Mediators. *Cell. Signalling*. **2021**, *78*, 109871.

[8] Mottaghitalab, F.; Kiani, M.; Farokhi, M.; Kundu, S.C.; Reis, R.L.; Gholami, M.; Bardania, H.; Dinarvand, R.; Geramifar, P.; Beiki, D.; Atyabi, F. Targeted Delivery System Based on Gemcitabine-Loaded Silk Fibroin Nanoparticles for Lung Cancer Therapy. *ACS Appl. Mater. Interfaces*. **2017**, *9*(37), 31600-31611.

[9] Ye, Z.C.; Huang, Y.M.; Ke, J.H.; Zhu, X.; Leng, S.L.; Luo, H. Breakthrough in Targeted Therapy for Non-small Cell Lung Cancer. *Biomed. Pharmacother.* **2021**, *133*, 111079.

[10]Liang, G.S.; Fan, W.G.; Luo, H.; Zhu, X. The Emerging Roles of Artificial Intelligence in Cancer Drug Development and Precision Therapy. *Biomed. Pharmacother.* **2020**, *128*, 110255.

[11]Busser, B.; Sancey, L.; Josserand, V.; Niang, C.; Favrot, M.C.; Coll, J-L.; Hurbin, A. Amphiregulin Promotes BAX Inhibition and Resistance to Gefitinib in Non-small-cell Lung Cancers. *Mol. Ther.* **2010**, *18*(3), 528-535.

[12]Wu, J.Y.; Wu, S.G.; Yang, C.H.; Chang, Y.L.; Chang, Y.C.; Hsu, Y.C.; Shih, J.Y.; Yang, P.C. Comparison of Gefitinib and Erlotinib in Advanced NSCLC and the Effect of EGFR Mutations. *Lung Cancer.* **2011**, *72*(2), 205-212.

[13]Serrano-Medina, A.; Oroz-Parra, I.; Gomez-Resendiz, V.E.; Licea-Navarro, A.; Licea-Claverie, A.; Cornejo-Bravo, J.M. Temperature- and pH-Sensitive Core-shell Nanogels as Efficient Carriers of Doxorubicin with Potential Application in Lung Cancer Treatment. *Int. J. Polym. Mater.* **2018**, *67*(1), 20-26.

[14]Zhou, X.; Li, R.; Chen, R.H.; Liu, J.J. Altered Mitochondrial Dynamics, Biogenesis, and Functions in the Paclitaxel-Resistant Lung Adenocarcinoma Cell Line A549/Taxol. *Med. Sci. Monit.* **2020**, *26*, e918216.

[15]Selvi, S.K.; Vinoth, A.; Varadharajan, T.; Weng, C.F.; Padma, V.V.. Neferine Augments Therapeutic Efficacy of Cisplatin through ROS-mediated Non-canonical Autophagy in Human Lung Adenocarcinoma (A549 cells). *Food Chem. Toxicol.* **2017**, *103*, 28-40.

[16]Ellerby, H.M.; Arap, W.; Ellerby, L.M.; Kain, R.; Pasqualini, R. Anti-cancer Activity of Targeted Pro-apoptotic Peptides. *Nat. Med.* **1999**, *5*(9), 1032-1038.

[17]Hao, X.Y.; Yan, Q.Y.; Zhao, J.; Wang, W.R.; Huang, Y.B.; Chen, Y.X. TAT Modification of Alpha-helical Anticancer Peptides to Improve Specificity and Efficacy. *PLoS One*. **2015**, *10*(9), e0138911.

[18]Kim, H.Y.; Kim, S.; Youn, H.; Youn, H.; Chung, J-K.; Shin, D.H.; Lee, K. The Cell Penetrating Ability of the Proapoptotic Peptide, KLAKLAKKLAKLAK Fused to the N-terminal Protein Transduction Domain of Translationally Controlled Tumor Protein MIIYRDLISH. *Biomaterials*. **2011**, *32*(22), 5262-5268.

[19]Feger, G.; Angelov, B.; Angelova, A. Prediction of Amphiphilic Cell-penetrating Peptide Building Blocks from Protein-derived Amino Acid Sequences for Engineering of Drug Delivery Nanoassemblies. *J. Phys. Chem. B*. **2020**, *124*, 4069-4078.

[20]Shteinfer-Kuzmine, A.; Amsalem, Z.; Arif, T.; Zooravlov, A.; Shoshan-Barmatz, V. Selective Induction of Cancer Cell Death by VDAC1-based Peptides and their Potential Use in Cancer Therapy. *Mol. Oncol*. **2018**, *12*(7), 1077-1103.

[21]Xiong, S.B.; Mu, T.Y.; Wang, G.W.; Jiang, X.J. Mitochondria-mediated Apoptosis in Mammals. *Protein Cell*. **2014**, *5*, 737-749.

[22]Wang, N.; Wang, W.; Huo, P.; Liu, C.Q.; Jin, J.C.; Shen, L.Q. Mitochondria-mediated Apoptosis in Human Lung Cancer A549 Cells by 4-methylsulfinyl-3-butenyl Isothiocyanate from Radish Seeds. *Asian Pac. J. Cancer Prev*. **2014**, *15*(5), 2133-2139.

[23]Yang, W. M.; Chen, Y.D.; Zhou, X.; Gu, Y.Z.; Qian, W.Q.; Zhang, F.; Han, W.; Lu, Tao.; Tang, W.F. Design, Synthesis and Biological Evaluation of Bis-aryl Ureas and Amides Based on 2-amino-3-purinylpyridine Scaffold as DFG-out B-Raf Kinase Inhibitors. *Eur. J. Med. Chem*. **2015**, *89*(7), 581-596.

[24]Derksen, M.; Vorwerk, C.; Siemen, D. Calpeptin, not Calpain, Directly Inhibits an Ion Channel of the Inner Mitochondrial Membrane. *Protoplasma*. **2016**, *253*, 835-843.

[25]Liu, D.; Angelova, A.; Liu, J.W.; Haramus, V.M.; Angelov, B.; Zhang, X.L.; Li. Y.W.; Li, N.; Zou, A.H. Self-assembly of Mitochondria-specific Peptide Amphiphiles Amplifying Lung Cancer Cell Death through Targeting the VDAC1-Hexokinase-II Complex. *J. Mater. Chem. B*. **2019**, *7*(30), 4706-4716.

[26]Chang, R.; Zou, Q.L.; Xing, R.R.; Yan, X.H. Peptide-Based Supramolecular Nanodrugs as a New Generation of Therapeutic Toolboxes against Cancer. *Adv. Ther*. **2019**, *2*(8), 1900048.

[27]Cao, S.J.; Xu, S.; Wang, H.M.; Ling, Y.; Dong, J.H.; Xia, R.D.; Sun, X.H. Nanoparticles: Oral Delivery for Protein and Peptide Drugs. *AAPS Pharmscitech*. **2019**, *20*, 190.

[28]Dinca, A.; Chien, W.M.; Chin, M.T. Intracellular Delivery of Proteins with Cell-Penetrating Peptides for Therapeutic Uses in Human Disease. *Int. J. Mol. Med*. **2016**, *17*, 263-275.

[29]Snyder, E.L.; Dowdy, S.F. Cell Penetrating Peptides in Drug Delivery. *Pharm. Res*. **2004**, *21*, 389-393.

[30]Aouacheria, A.; Cibiel, A.; Guillemin, Y.; Gillet, G.; Lalle, P. Modulating Mitochondria-mediated Apoptotic Cell Death through Targeting of Bcl-2 Family Proteins. *Recent Pat. DNA Gene Sequences*. **2007**, *1*(1), 43-61.

[31]Goldsmith, K.C.; Liu, X.; Dam, V.; Morgan, B.T.; Shabbout, M.; Cnaan, A.; Letai, A.; Korsmeyer, S.J.; Hogarty, M.D. BH3 Peptidomimetics Potently Activate Apoptosis and

Demonstrate Single Agent Efficacy in Neuroblastoma. *Oncogene*. **2006**, *25*(33), 4525-4533.

[32]Pastorino, J.G.; Shulga, N.; Hoek, J.B. Mitochondrial Binding of Hexokinase II Inhibits Bax-induced Cytochrome c Release and Apoptosis. *J. Biol. Chem.* **2002**, *277*, 7610-7618.

[33]Majewski, N.; Nogueira, V.; Bhaskar, P.; Coy, P.E.; Skeen, J.E.; Gottlob, K.; Chandel, N.S.; Thompson, C.B.; Robey, R.B.; Hay, N. Hexokinase-mitochondria Interaction Mediated by Akt Isrequired to Inhibit Apoptosis in the Presence or Absence of Bax and Bak. *Mol. Cell*. **2004**, *16*(5), 819-830.

[34]Woldetsadik, A.D.; Vogel, M.C.; Rabeh, W.M.; Magzoub, M. Hexokinase II-derived Cell-Penetrating Peptide Targets Mitochondria and Triggers Apoptosis in Cancer Cells. *FASEB J*. **2017**, *31*, 2168-2184.

[35]Chiara, F.; Castellaro, D.; Marin, O.; Petron, V.; Brusilow, W.S.; Juhaszova, M.; Sollott, S.J.; Bernardi, P.; Rasola, A. Hexokinase II Detachment from Mitochondria Triggers Apoptosis through the Permeability Transition Pore Independent of Voltage-Dependent Anion Channels. *PLoS One*. **2008**, *3*(3), e1852.

[36]Zaid, H.; Abu-Hamad, S.; Israelson, A.; Nathan, I.; Shoshan-Ba, V. The Voltage-dependent Anion Channel-1 Modulates Apoptotic Cell Death. *Cell Death Differ*. **2005**, *12*(7), 751-760.

[37]Palanikumar, L.; Al-Hosani, S.; Kalmouni, M.; Saleh. O.; Magzoub, M. Hexokinase II-Derived Cell-Penetrating Peptide Mediates Delivery of MicroRNA Mimic for Cancer-Selective Cytotoxicity. *Biochemistry*. **2020**, *59*, 2259-2273.

[38]Zhang, Z.Y.; Sun, G.C.; Chen, W.; Su, J.H.; Tian, H. The Endeavor of Vibration-induced Emission (VIE) for Dynamic Emissions. *Chem. Sci.* **2020**, *11*, 7525-7537.

[39]Humeniuk, H.V.; Rosspeintner, A.; Licari, G.; Licari, G.; Licari, G.; Kilin, V.; Bonacina, L.; Vauthey, E.; Sakai, N.; Matile, S. White-fluorescent Dual-emission Mechanosensitive Membrane Probes that Function by Bending Rather than Twisting. *Angew. Chem.-Int. Edit.* **2018**, *130*(33), 10719-10723.

[40]Huang, W.; Sun, L.; Zheng, Z.; Su, J.H.; Tian, H. Colour-tunable Fluorescence of Single Molecules Based on the Vibration Induced Emission of Phenazine. *Chem Comm.* **2015**, *51*(21), 4462-4464.

[41]Zhang, Y.; Li, Y.; Wang, H.; Zhang, Z.Y.; Feng, Y.L.; Tian, Q.; Li, N.; Mei, J.; Su, J.H.; Tian, H. Measuring the Microphase Separation Scale of Polyurethanes with a Vibration-Induced Emission-Based Ratiometric "Fluorescent Ruler". *ACS Appl. Mater. Interfaces*. **2019**, *11*(42), 39351-39358.

[42]Richter, R.P.; Berat, R.; Brisson, A. R. Formation of Solid-Supported Lipid Bilayers: An Integrated View. *Langmuir*. **2006**, *22*(8), 3497−3505.

[43]Li, Y.W.; Angelova, A.; Hu, F.Z.; Garamus, V.M.; Peng, C.J.; Li, N.; Liu, J.W.; Liu, D.; Zou, A.H. pH Responsiveness of Hexosomes and Cubosomes for Combined Delivery of Brucea javanica Oil and Doxorubicin. *Langmuir*. **2019**, *35*, 14532-14542.

[44]Lu, X.L.; Shi, R.X.; Hao, C.C.; Chen, H.; Zhang, L.; Li, J.H.; Xu, G.Q.; Sun, R.G. Behavior of Lysozyme Adsorbed onto Biological Liquid Crystal Lipid Monolayer at the Air/Water Interface. *Chinese Phys B*. **2016**, *25*(9), 49-55.

[45]He, G.X.; Sun, R.G.; Hao, C.C.; Yang, J.; Wang, M.; Zhang, L.N. Thermodynamic

Analysis and AFM Study of the Interaction of Palmitic Acid with DPPE in Langmuir Monolayers. *Colloids Surf. A Physicochem. Eng. Asp*. **2014**, *441*(20), 184-194.

[46]Kurek, J.; Boczoń, W.; Myszkowski, K.; Murias, M.; Borowiak, T.; Wolska, I. Synthesis of Sulfur Containing Colchicine Derivatives and their Biological Evaluation as Cytotoxic Agents. *Lett. Drug Des. Discov*. **2014**, *11*(3), 279-289.

[47]Weniger, M.A.; Rizzatti, E.G.; Perez-Galan, P.; Liu, D.L.; Wang, Q.Y.; Munson, P.J.; Raghavachari, N.; White, T.; Tweito, M.M.; Dunleavy, K. Treatment-Induced Oxidative Stress and Cellular Antioxidant Capacity Determine Response to Bortezomib in Mantle Cell Lymphoma. *Clin. Cancer Res*. **2011**, *17*(15), 5101-5112.

[48]Ikematsu, H.; Kawai, N.; Iwaki, N.; Kashiwagi, S.; Ishikawa, Y.; Yamaguchi, H.; Shiosakai, K. In Vitro Neuraminidase Inhibitory Concentration (IC_{50}) of Four Neuraminidase Inhibitors in the Japanese 2015–16 Season: Comparison with the 2010–11 to 2014–15 Seasons. *J. Infect. Chemother*. **2018**, *24*(9), 707-712.

[49]Poncelet, L.; Garigliany, M.; Ando, K.; Franssen, M.; Desmecht, D.; Brion, J.P. Cell Cycle S Phase Markers are Expressed in Cerebral Neuron Nuclei of Cats Infected by the Feline Panleukopenia Virus. *Cell Cycle*. **2016**, *15*(24), 3482-3489.

[50]Nicol, S.M.; Bray, S.E.; Black, H.D.; Lorimore, S.A.; Wright, E.G.; Lane, D.P.; Meek, D.W.; Coates, P.J.; Fuller-Pace, F.V. The RNA Helicase p68 (DDX5) is Selectively Required for the Induction of p53-dependent p21 Expression and Cell-cycle Arrest after DNA Damage. *Oncogene*. **2013**, *32*, 3461-3469.

[51]Chen, L.M.; Li, G.D.; Peng, F.; Jie, X.M.; Dongye, G.Z.; Cai, K.G.; Feng, R.B.; Li, B.J.; Zeng, Q.W.; Lun, K.Y.; Chen, J.C.; Xu, B.L. The Induction of Autophagy Against

Mitochondria-mediated Apoptosis in Lung Cancer Cells by a Ruthenium (II) Imidazole Complex. *Oncotarget*. **2016**, *7*(49), 80716-80734.

[52]Mallick, S.; Thuy, L.T.; Lee, S.; Park, J-II.; Choi, J.S. Liposomes Containing Cholesterol and Mitochondria-penetrating Peptide (MPP) for Targeted Delivery of Antimycin A to A549 cells. *Colloids Surf. B*. **2018**, *161*, 356-364.

[53]Sun, Y.; Chen, Y.Y.; Ma, X.Y.; Yuan, Y.; Liu, C.S.; Kohn, J.; Qian, J.C. Mitochondria-Targeted Hydroxyapatite Nanoparticles for Selective Growth Inhibition of Lung Cancer in Vitro and in Vivo. *ACS Appl. Mater. Interfaces*. **2016**, *8*, 25680-25690.

[54]Sun, X.; Zhong, Y.; Luo, H.T.; Yang, Y.F. Selenium-Containing Polysaccharide-Protein Complex in Se-Enriched Ulva fasciata Induces Mitochondria-Mediated Apoptosis in A549 Human Lung Cancer Cells. *Mar. Drugs*. **2017**, *15*(7), 215.

[55]Wang, F.Y.; Tang, X.M.; Wang, X.; Huang, K.B.; Feng, H.W.; Chen, Z.F.; Liu, Y.N.; Liang, H. Mitochondria-targeted Platinum (II) Complexes Induce Apoptosis-dependent Autophagic Cell Death Mediated by ER-stress in A549 Cancer Cells. *Eur. J. Med. Chem*. **2018**, *155*, 639-650.

[56]Tan, G.X.; Uson-Lopez, R.A.; Rahman, M.M.; Hosokawa, T.; Saito, T.; Kurasaki, M. Myricetin Enhances on Apoptosis Induced by Serum Deprivation in PC12 Cells Mediated by Mitochondrial Signaling Pathway. *Environ. Toxicol. Pharmacol*. **2018**, *57*, 175-180.

[57]Li, X.T.; Xie, H.Q.; Chen, Y.J.; Lang, M.Z.; Chen, Y.Y.; Shi, L.G. Silkworm Pupa Protein Hydrolysate Induces Mitochondria-Dependent Apoptosis and S Phase Cell Cycle Arrest in Human Gastric Cancer SGC-7901 Cells. *Int. J. Mol. Med*. **2018**, *19*(4),

1013.

[58]Lin, P.Y.; Tsai, C.T.; Chuang, W.L.; Chao, Y.H.; Pan, I.H.; Chen, Y.K.; Lin, C.C.; Wang, B.Y. Chlorella Sorokiniana Induces Mitochondrial-mediated Apoptosis in Human Non-small Cell Lung Cancer Cells and Inhibits Xenograft Tumor Growth in Vivo. *BMC Complementary Altern. Med.* **2017**, *17*, 88.

Table of Contents graphic: